http://dx.doi.org/10.5012/bkcs.2012.33.3.869

Pharmacophore Modeling and Molecular Dynamics Simulation to Find the Potent Leads for Aurora Kinase B†

Sugunadevi Sakkiah, Sundarapandian Thangapandian, Yongseong Kim,‡ and Keun Woo Lee*

*Division of Applied Life Science (BK21 Program), Systems and Synthetic Agrobiotech Center (SSAC), Plant Molecular Biology and Biotechnology Research Center (PMBBRC), Research Institute of Natural Science (RINS), Gyeongsang National University (GNU), Jinju 660-701, Korea. *E-mail: kwlee@gnu.ac.kr*
‡Department of Science Education, Kyungnam University, Masan 631-701, Korea
Received December 20, 2011, Accepted January 3, 2012

Identification of the selective chemical features for Aurora-B inhibitors gained much attraction in drug discovery for the treatment of cancer. Hence to identify the Aurora-B critical features various techniques were utilized such as pharmacophore generation, virtual screening, homology modeling, molecular dynamics, and docking. Top ten hypotheses were generated for Aurora-B and Aurora-A. Among ten hypotheses, HypoB1 and HypoA1 were selected as a best hypothesis for Aurora-B and Aurora-A based on cluster analysis and ranking score, respectively. Test set result revealed that ring aromatic (RA) group in HypoB1 plays an essential role in differentiates Aurora-B from Aurora-A inhibitors. Hence, HypoB1 used as 3D query in virtual screening of databases and the hits were sorted out by applying drug-like properties and molecular docking. The molecular docking result revealed that 15 hits have shown strong hydrogen bond interactions with Ala157, Glu155, and Lys106. Hence, we proposed that HypoB1 might be a reasonable hypothesis to retrieve the structurally diverse and selective leads from various databases to inhibit Aurora-B.

Key Words : Aurora kinase, Pharmacophore, Molecular dynamics, Homology modeling, Molecular docking

Introduction

The serine/threonine family of Aurora kinases plays an important role in cell cycle.[1] Several pharmaceutical companies and research industries mainly focused on Aurora kinases due to its major role in regulating the mitosis and cytokinesis.[2] Mitosis is a vital process for the regeneration of tissues and genomic development of an individual as well as functional integrity of a cell.[3] To date, three Homo sapiens Aurora kinases are identified: Aurora-A, -B, and -C, the biology of these have been reviewed extensively. These three kinases show 67-76% sequence identity in their catalytic domains however depict a small variation in N-terminal domain.[4,5] The N-terminal domain shares a low sequence conservation and determines the selectivity during protein-protein interaction.[4] The C-terminal domain of human Aurora-B shares 53% and 73% sequence similarity to human Aurora-A and C, respectively.[6] The active site cleft is bounded by the glycine-rich loop which contains the consensus kinase sequence Gly-X-Gly-X-X-Gly and activation loop. All three Aurora kinases influence the cell cycle from its G2 phase through cytokinesis as well as appear at specific locations during mitosis: (i) Aurora-A, localizes on centrosomes, primarily associated with the centrosomes separation[7,8] (ii) Aurora-B, a chromosomal passenger protein localizes at centromeres during the prometaphases and subsequently relocates to midzone microtubules and midbodies during the anaphase and telophase[9,10] (iii) Aurora-C highly expressed in testis and plays a role in spermatigeneis and act as a chromosomal passenger.[11-13]

Aurora kinases are strongly associated with human cancer[14-16] and over-expression of Aurora-A and Aurora-B leads to many cancers such as colon,[17] breast,[18] prostate,[13] pancreas,[19] thyroid,[20] head,[21] and neck.[22] Aurora-A, proposed to function in late anaphase, promoting spindle elongation, centrosome separation, and spindle bipolarity. Over-expression of Aurora-A disrupt the assembly of the mitotic checkpoint complex that leads to the genetic instability and tumorigenesis.[23] Dysregulation of Aurora-A is thought to be oncogenic and resulted in the production of multiple centrosomes and aneuploidy.[18,24] Aurora-A selective inhibition results in mitosis accumulation and abnormalities in centrosome separation leading to the formation of monopolar spindles. Over-expression of Aurora-B correlates with the clinical stages in primary colon cancer and closely implicated in tumor progression.[15] Due to the inhibition of Aurora-B activity in tumor cells, the cells are forced through a catastrophic mitotic exit which leads to polypoid cells that rapidly lose viability. Aurora-B phosphorylates the serine 10 of histone H3 and inhibits its function induces an anti-proliferative phenotype indicates that Aurora-B as an attractive anti-cancer drug target.[1,25,26] Examination of the relationship between Aurora-C and cancer is limited; however several studies have been reported that aberrant expression of Aurora-C in colorectal, breast, and prostate cancer.[12]

Recent elucidation of the biological function of Aurora kinases in normal and cancer cells had led to the develop-

†This paper is to commemorate Professor Kook Joe Shin's honourable retirement.

ment of small-molecule inhibitor. Aurora-A and Aurora-B are investigated as potential targets for anticancer therapy.[27] Inhibition of either Aurora-A or Aurora-B yields distinct phenotypes; hence it may present two avenues for anticancer drug discovery.[18] Development of inhibitors against Aurora kinases as anticancer molecules gained attention because of the facts that aberrant expression of Aurora kinases leads to chromosomal instability, derangement of multiple tumor suppressor, and oncoprotein regulated pathways.[27] These observations suggest that inhibition of one or more Aurora kinases might be a promising molecular target for the cancer treatment. Thus, scientists articulate a concern to design selective inhibitors for Aurora kinases. Designing a selective inhibitor for Aurora kinases will be one of the challenging tasks in cancer research field since its similarities in the primary and secondary structures. Mainly the ATP-binding domain of Aurora kinase is major target for the current growth of new classes of anti-cancer drug. Therefore, it has a considerable interest in developing a specific and novel anti-cancer drugs to achieve the selectivity between Aurora-B and Aurora-A.[2]

In this work we mainly focused on the chemical features which can differentiate the Aurora-B from Aurora-A. Common feature hypothesis was generated and performed a systematic comparison of the pharmacophore models for Aurora-B and Aurora-A. In order to find the selective 3D pharmacophoric features for Aurora-B and Aurora-A inhibitors the best hypothesis was selected for Aurora-B and Aurora-A and compared to find the critical chemical features which can differentiate the Aurora-B and Aurora-A inhibitors. The selected best models were validated using test set which consists of structurally diverse and selective inhibitors of Aurora-B and Aurora-A. The resultant pharmacophore model was used as an input in the virtual screening and the hit compounds were filtered out by applying the Lipinski's rule of five and ADMET properties. Homology modeling and Molecular Dynamics (MD) simulations were carried out to generate a 3D structure of human Aurora-B. The sorted hit molecules were subjected to molecular docking studies to find a suitable orientation in the active site of Aurora-B.

Methods and Materials

Molecules Preparation to Generate and Validate the Hypothesis. To generate the qualitative hypothesis for Aurora-A and Aurora-B, training set A and B are prepared by selecting 10 and 4 known selective inhibitors based on the receptor binding activity of Aurora-A[1,28,29] and Aurora-B,[30-34] respectively. The 2D format of all molecules were built using MDL-ISIS Draw and converted into 3D using Discovery Studio v2.5 (DS, www.accelrys.com). For minimization, a maximum number of 255 conformations were generated for each compound using *Best Conformation model* generation method by applying CHARMm force field and Poling algorithm.[35] To assure the energy-minimized conformation, the conformations with energy higher than 20 $kcal^{-1}mol^{-1}$ from the global minimum were rejected. The molecules with their good conformation (lowest energy) are used to generate the hypothesis.[36,37] The best conformation models were used not only for hypothesis generation but also to find how well the molecules fit in the generated hypothesis. Test set was used to validate the generated hypotheses which consist of 19 molecules (10 selective Aurora-B and 9 selective Aurora-A inhibitors).

Qualitative Hypothesis Generation. Ligand-based approach is one of the most powerful tools in rational drug design process. Hence, qualitative hypotheses were generated for Aurora-B and Aurora-A based on the selective inhibitors in training sets. There are two main strategies to generate the quantitative hypothesis: (i) assumes all the compounds present in the training set are important and contains vital features (ii) gives bias to the most active compounds assuming that they contain important features.[38] In this work, Hip-Hop algorithm was used to generate the common feature hypothesis to find the important chemical features shared by a set of selective Aurora kinase inhibitors. Hip-Hop algorithm was performed in three-steps:[39] (i) generate a conformation models for each molecule in the training set, (ii) each conformer is examined by the presence of certain chemical features, and (iii) a three-dimensional configuration of chemical features common to the input molecules were determined. DS provides a dictionary of important chemical features in drug-enzyme/receptor interactions such as hydrogen bond acceptor (HBA), hydrogen bond donor (HBD), hydrophobic group (HY), ring aromatic (RA) and positive (PI) and negative ionizable (NI) groups. HBA, HBD, HY, and RA features are selected, to design the pharmacophore models for Aurora-B based on the chemical features present in the selective and active inhibitors of Aurora-B (training set). The chemical features like HBA, HBD, and HY were selected to generate the Aurora-A hypothesis based on the reported pharmacophore model by Deng *et al.*.[40]

In the hypothesis generation methodology all the parameters are kept constant except the following: highest weight value of 2 was assigned for the most active compound (ensures that all the chemical features present in the compound could be considered in building hypothesis). A value of "1" for the principle column ensures that at least one map for each of generated hypotheses will be found and a value of "1" for the maximum omitting features column ensures that all but one feature must description of these input parameters. Applying the above parameters top ten common features hypotheses were generated from the training set based on the ranking scores. The ranking score is a measure of how well the molecules map onto the produced pharmacophore models as well as the rarity of the pharmacophore model.

Selection of Best Pharmacophore Models. Cluster analysis was performed based on the chemical features composition to select the best hypothesis for Aurora-A and Aurora-B. Following are the strategies adopted to select a best hypothesis from top ten hypotheses of Aurora-B and

Aurora-A: (i) clustering analysis: based on their ranking score and composition similarities, (ii) all training sets compounds were selected to validate the lustiness and selectivity of a top ranked hypothesis from each cluster using "*Ligand Pharmacophore Mapping*", and (iii) test sets: includes selective inhibitors of Aurora-B and Aurora-A with a wide structural diversity. Test was used to identify the best model that can accurately distinguish Aurora-B and Aurora-A inhibitors as well as to evaluate the robustness and selectivity of best pharmacophore models. The hypothesis quality was predicted by calculating the "fit-value" and this value is defined as the weight (f) X [1-SSE (f)], where f is the mapping features, SSE (f) is the sum over location constraints c on f of [D(c)/T(c)] 2, D is the displacement of the feature from the center of the location constraint, and T (tolerance) is the radius of the location constraint sphere for the feature. Thus, the maximum fit value for a perfectly fitting compound is the sum of weight values for all features and the minimum value should be 0. Finally, to figure out the key chemical features exciting in hypothesis that contributed the most selectivity's towards the specific target.

Virtual Screening of Chemical Database. Virtual screening of database can serve for two main purposes: (i) to validate the quality of generated pharmacophore models by selective detection of compounds with known inhibitory activity and (ii) to find novel and potential leads suitable for particular target. The best hypothesis which can differentiate Aurora-B inhibitors from Aurora-A was used as an input in *Ligand Pharmacophore mapping* to retrieve the new leads from two different chemical databases such as Maybridge (60,000) and Chembridge (50,000). The screened molecules were further filtered based on top 10% from the total hits, then Lipinski's rule of five, and ADMET properties were calculated to refine the retrieved hits. Finally, the molecules which pass all the filtrations were subjected to molecular docking study to find the suitable binding orientation in active site of Aurora-B.

Homology Modeling of Aurora-B. Homology or comparative modeling is one of the most accurate computational techniques to generate a reliable tertiary structure from primary structure of proteins and routinely used in many biological applications. Due to the lack of 3D structure of human Aurora-B, homology model was generated using the highly conserved template deposited in Protein Data Bank (PDB). Human Aurora-B primary sequence (344 amino acids) was retrieve from Swiss-Prot Protein Database (Accession ID: Q96GD4). The identification of suitable template protein is one of the important steps in homology modeling. The identity and similarity between target and template proteins determine the quality of the predicted structure. Hence to find a suitable template for Aurora-B, a similarity search against PDB was performed using BLAST server. Three dimensional structure of Aurora-B was built using MODELLER algorithm implemented in *Build Homology Module/DS* based on 3D structure of *Xenopus laevis* Aurora-B. The final model was evaluated using the PROCHECK program,[41] to search for deviations from normal protein conformational parameters.

Molecular Dynamics Validation for Modeled Aurora-B. MD simulation was performed using GROMACS v 3.3,[42] to gain a better relaxation and a correct arrangement of the atoms as well as to refine the side chain orientation of Aurora-B model, by applying GROMACS force field.[42-44] The model was solvated in a cubic box of dimension 1 nm and SPC water model used to create aqueous environment. Particles mesh Ewald (PME)[45] electrostatic and periodic boundary conditions were applied in all directions. The system was neutralized by adding 8 Cl^- counter ions by replacing 8 water molecules. It was subjected to a steepest descent energy minimization until a tolerance of 1000 $kj{\cdot}mol^{-1}$, step by step to avoid the high energy interactions and steric clashes. All the bond lengths were constrained with the LINCS[46] method and energy minimized system are treated for 100 ps equilibration run. The pre-equilibrated system was consequently subjected to 5 ns production MD simulation, with a time-step of 2 fs at constant temperature (300 K), pressure (1 atm) and without any position restraints.[47] Snapshots were collected for every 5 ps and the analysis of the MD simulation was carried out by GROMACS analysis tools. From the 5 ns MD simulation, the representative structure was selected as a best model for further studies.

Molecular Docking Protocol. In computer-aided drug design, molecular docking was used as a post filtration process to find the suitable binding orientation (poses) of ligands in protein active site. The quality of receptor structure plays a central role in determining the success of docking calculations.[39] In general, higher resolution of the employed crystal structure, better observed docking results. Hence, the validated homology structure of Aurora-B was used as a receptor for molecular docking studies. *LigandFit* module was used to dock the training set compounds as well the database hit compounds. There are three stages in *LigandFit* protocol: (i) Docking: attempt is made to dock a ligand into a user defined binding site, (ii) In-Situ Ligand Minimization, and (iii) Scoring: various scoring functions were calculated for each pose of the ligands. For docking study initially CHARMm force field was applied for Aurora-B using *Receptor-Ligand Interactions* tool.

After the protein preparation the active site of the protein has to be identified to dock the small molecules. The active site also represented as binding site; it's a set of points on a grid that lie in a cavity. Two methods are applied to define a protein binding site: (i) eraser algorithm defines the active site based on the shape of the receptor and (ii) volume occupied by the known ligand in the active site. For this study, first method was applied to find the active site of Aurora-B (Homology model) and well know specific 11 Aurora-B inhibitors were docked at the binding site of Aurora-B. During the docking process, the best top 10 ligands conformations were generated based on dock score value after the energy minimization using the smart minimizer method (steepest descent method and followed by the conjugate gradient method).

Results and Discussions

The accurate prediction of binding affinities and biochemical activities of small molecules (agonist/antagonist) is one of the major challenges in computational drug design approaches.[36] Indirect ligand-based and direct receptor-based approaches were used to determine the structure-activity relationship of small molecules. Utilizing the above knowledge to identify new molecules with greater activity and better selectivity towards specific target.[39] Therefore, ligand-based pharmacophore modeling based virtual screening and molecular docking study were carried to find critical chemical features responsible to differentiate Aurora-B from Aurora-A inhibitors.

Generation of Aurora-B Hypothesis. Based on the training set B (Fig. 1(a)), top 10 ranked common feature hypotheses (HypoB1-HypoB10) were generated according to their ranking scores from 35.41 to 25.04. Direct hit and partial hit mask value of '1' and '0' for all hypotheses indicates that all the molecules mapped well with the chemical features present in hypothesis and there is no partial mapping or missing feature in training set molecules, respectively (Table 1). The top ranked HypoB1 consist of HY, RA, and two HBA chemical features (Fig. 2(a)) and the remaining all hypotheses demonstrate a lesser score value when compared with HypoB1. Comparing all ten hypotheses, it was classified into two groups based on the number of chemical features: Group I contain four chemical features (HypoB1 to HypoB4, and HypoB6) and Group II consists of three chemical features (HypoB5 and HypoB7 to HypoB10).

The difference between pharmacophoric features and its locations as well as the composition can be evaluated and categorized using *Hypothesis clustering* module from Catalyst v4.11. Based on the chemical features similarity, the generated top 10 hypotheses were clustered into three groups (Table 2). Cluster I, comprises four hypotheses such as HypoB1, HypoB4 from Group I and HypoB8, HypoB10 from Group II. The Hypotheses in Group I, HypoB1, contains 1-RA, 1-HY, and 2-HBA features and HypoB4 comprises 2-HY and 2-HBA chemical features and Group II contains 1-HY and 2-HBA chemical features. Cluster II has five hypotheses such as HypoB2, HypoB3, HypoB6 from Group I and HypoB5, HypoB9 from Group II. In Group I, HypoB2 and HypoB3 have similar and common chemical features like 1-RA, 2-HY, and 1-HBA but HypoB6 consist of 3-HY and 1-HBA groups. Both the hypothesis in Group II contains similar chemical features like 1-RA, 1-HY, and 1-

Table 1. Details of the top ten hypotheses generated using Hip-Hop for Aurora-B

Hypothesis	Features[a]	Ranking[b]	Direct Hit[c]	Partial Hit[d]
HypoB1	RA, HY, HBA, HBA	35.410	1111	0000
HypoB2	R, HY, HY, HBA	32.914	1111	0000
HypoB3	RA, HY, HY, HBA	32.914	1111	0000
HypoB4	HY, HY, HBA, HBA	32.772	1111	0000
HypoB5	RA, HY, HBA	31.757	1111	0000
HypoB6	HY, HY, HY, HBA	29.704	1111	0000
HypoB7	RA, RA, HBA	26.177	1111	0000
HypoB8	HY, HBA, HBA	25.675	1111	0000
HypoB9	RA, HY, HBA	25.043	1111	0000
HypoB10	HY, HBA, HBA	25.042	1111	0000

[a]RA = Ring aromatic; HBA = Hydrogen Bond Acceptor; HBD = Hydrogen Bond Donor; HY = Hydrophobic. [b]Higher the ranking score, lesser the probability of chance correlation. The best hypothesis shows the highest value. [c,d]DH, PH indicates whether (1) or (0) a training set molecule mapped every feature of the hypothesis and mapped to all but one feature in the hypothesis. The numbers from (right to left) correspond to the compounds (from top to bottom).

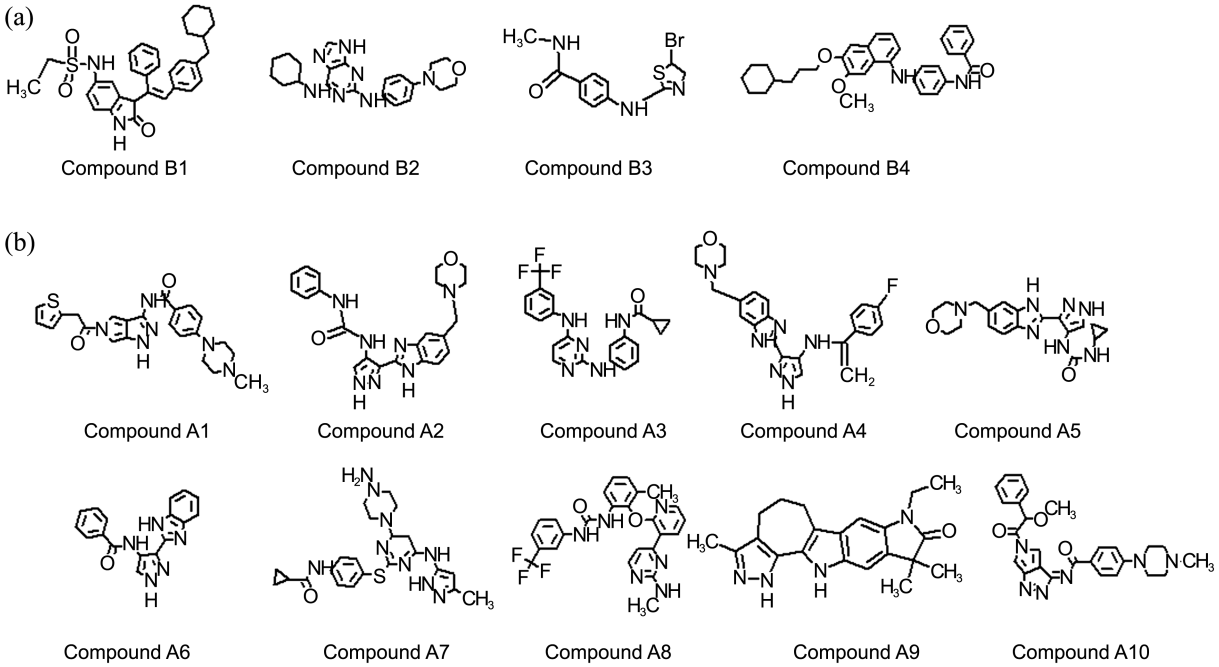

Figure 1. (a) Structure of Aurora-B inhibitor for the Hip-Hop training set B (b) Structure of Aurora-A inhibitor for the Hip-Hop training set A.

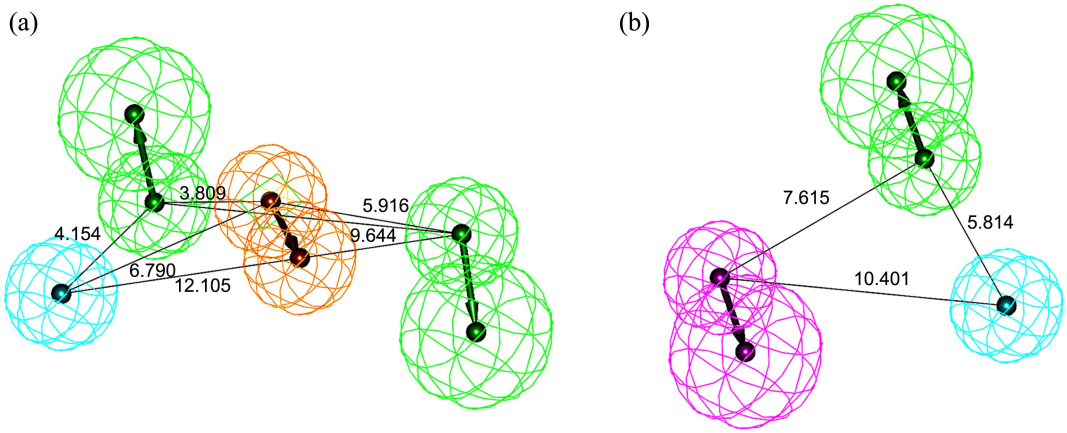

Figure 2. Geomentric constraints of (a) HypoB1 (b) HypoA1. Green:HBA (Hydrogen bond acceptor); Brown: RA (Ring aromatic); and Cyan: HY (Hydrophobic).

HBA chemical group. Only one hypothesis was present in Cluster III from Group II that contains 2-RA and 1-HBA features.

Analyzing the Cluster I and II, we identified that the Group I hypotheses shows a good ranking score of above 30 when compared with the Group II which shows the ranking score value approximately 25. However, one hypothesis from Group II shows the ranking score value of 31 (HypoB5) and HypoB6 from Group I shows the value less than 30. Thus for further analysis we selected HypoB1, HypoB4 and HypoB2, HypoB5 hypotheses from Cluster I and Cluster II, respectively. HypoB3 was not included in the further process hence it proposed a similar geometric constraints, chemical features, and ranking score.

Comparing all four hypotheses, 1-HBA and 1-HY chemical groups are present commonly in all hypotheses. The remarkable change was observed in ranking score due to the addition of RA and HBA group combined with 1-HBA and 1-HY features. When RA was combined with common chemical features like 1-HBA and 1-HY the ranking score value was 31, this was observed from HypoB5. The addition of 1-RA and 1-HY or 1-HY and 1-HBA groups with common chemical features (1-HBA and 1-HY) shows the ranking score increased to 32 (HypoB2, HypoB4) than HypoB5. The combination of 2-HY, 2-HBA and 1-RA, 2-HY, and 1-HBA shows the similar ranking score value of 32. Interestingly, the ranking score of HypoB1 (35.41) was high due to the combination of 1-RA and 1-HBA with 1-Hy and 1-HBA. Hence, HypoB1 was selected as best hypothesis and we proposed that the 1-RA and 1-HBA could be important to select potent inhibitors of Aurora-B. Figure 3(a) shows how well the chemical features present in CompoundB1 (Fit Value = 3.73) mapped with the selected best hypothesis HypoB1.

Table 2. Summary of Hypotheses for Aurora-B kinase receptor antagonists

Hypothesis[a]	Ranking score[b]	Features[c]	Cluster[d]
HypoB1	35.410	RA, HY, HBA, HBA	I
HypoB4	32.772	HY, HY, HBA, HBA	
HypoB8	25.675	HY, HBA, HBA	
HypoB10	25.042	HY, HBA, HBA	
HypoB5	31.757	RA, HY, HBA	
HypoB3	32.914	RA, HY, HY, HBA	II
HypoB2	32.914	RA, HY, HY, HBA	
HypoB9	25.043	RA, HY, HBA	
HypoB6	29.704	HY, HY, HY, HBA	
HypoB7	26.177	RA, RA, HBA	III

[a]Numbers for the hypothesis are consistent with the numeration as obtained by the hypothesis generation. [b]The higher the ranking score, the less likely is it that the molecules in the training set fit the hypothesis by a chance correlation. The best hypotheses have the highest ranks. [c]RA = ring aromatic; HY = hypdophobic group; HBA = hydrogen bond acceptor group; HBD = hydrogen bond donor group. [d]Cluster assembly is adopted from Catalyst's "hypotheses clustering analysis result based on the composition similarity between hypotheses.

Generation of Aurora-A Hypothesis. Top ten qualitative hypotheses were generated based on the common features present in the training set A (Fig. 1(b)). All hypotheses contained HY and HBD groups which indicated that these two features are very important for Aurora-A activity (Table 3). The top 10 hypotheses (HypoA1-HypoA10) showed the scores range from 69.95 to 60.78. Cluster analysis was performed; ten hypotheses were classified into three clusters based on the chemical features (Table 4). Cluster I contains 8 hypotheses, all having the same chemical features, the difference between each hypothesis lies in the 3D arrangement of pharmacophoric features. Cluster II and III contains one hypothesis each.

Figure 3(b) shows the alignment represent how well the CompoundA1 mapped with HypoA1, using the "*Ligand Pharmacophore Mapping*" method. During the fit process the conformations of CompoundA1 were minimized within the 20 kcal/mol energy threshold to minimize the distance between HypoA1 features and mapped atoms of CompoundA1 Alignment of all training set was performed and found to give fit score from 3.0 to 1.64. In this study, the highest ranked pharmacophore hypothesis HypoA1 from Cluster I was selected as a statistically best hypothesis, it maps to all the important features of the active compounds

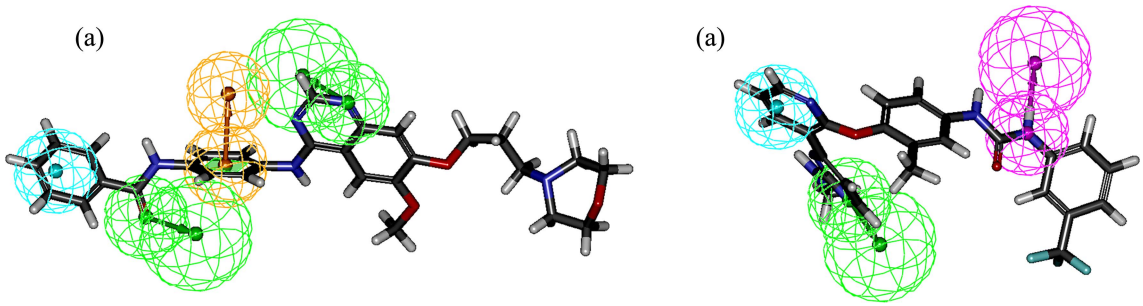

Figure 3. (a) CompoundB1 shows a best alignment with HypoB1 hypothesis. (b) CompoundA1 shows a best alignment with HypoA1 hypothesis.

Table 3. Details of the top ten hypotheses generated using Hip-Hop for Aurora-A

Hypothesis	Features[a]	Ranking[b]	Direct Hit[c]	Partial Hit[d]
HypoA1	HY, HBA, HBD	69.951	1111111111	0000000000
HypoA2	HY, HBA, HBD	67.921	1111111111	0000000000
HypoA3	HY, HBA, HBD	67.276	1111111111	0000000000
HypoA4	HY, HBA, HBD	66.868	1111111111	0000000000
HypoA5	HY, HBA, HBD	66.093	1111111111	0000000000
HypoA6	HY, HBA, HBD	63.633	1111111111	0000000000
HypoA7	HY, HBA, HBA	62.265	1111111111	0000000000
HypoA8	HY, HBA, HBD	61.503	1111111111	0000000000
HypoA9	HY, HY, HBD	60.982	1111111111	0000000000
HypoA10	HY, HBA, HBD	60.789	1111111111	0000000000

[a]HBA = Hydrogen Bond Acceptor; HBD = Hydrogen Bond Donor; HY = Hydrophobic. [b]Higher the ranking score, lesser the probability of chance correlation. The best hypothesis shows the highest value. [c,d]DH, PH indicates whether (1) or (0) a training set molecule mapped every feature of the hypothesis and mapped to all but one feature in the hypothesis. The numbers from (right to left) correspond to the compounds (from top to bottom).

Table 4. Summary of Hypotheses for Aurora-A kinase receptor antagonists

Hypothesis[a]	Ranking score[b]	Features[c]	Cluster[d]
HypoA1	69.951	HY, HBA, HBD	I
HypoA8	61.503	HY, HBA, HBD	
HypoA4	66.868	HY, HBA, HBD	
HypoA2	67.921	HY, HBA, HBD	
HypoA5	66.093	HY, HBA, HBD	
HypoA3	67.276	HY, HBA, HBD	
HypoA10	60.789	HY, HBA, HBD	
HypoA6	63.633	HY, HBA, HBD	
HypoA9	60.982	HY, HY, HBD	II
HypoA7	62.265	HY, HBA, HBA	III

[a]Numbers for the hypothesis are consistent with the numeration as obtained by the hypothesis generation. [b]The higher the ranking score, the less likely is it that the molecules in the training set fit the hypothesis by a chance correlation. The best hypotheses have the highest ranks. [c]HY = hydophobic group; HBA = hydrogen bond acceptor group; HBD = hydrogen bond donor group. [d]Cluster assembly is adopted from Catalyst's "hypotheses clustering analysis result based on the composition similarity between hypotheses.

and to some extent shows correlation between best fit values, conformational energies and actual activities of the training set A in comparison to other hypotheses.

Table 5. Test Set A for HypoA1

Name	Fit Values		IC_{50} Values	
	Hypo1A	Hypo1B	Aurora A	Aurora B
Test1	2.990	3.687	0.450	0.002
Test2	2.947	3.460	0.220	0.001
Test3	2.991	3.590	0.410	0.002
Test4	2.975	3.593	0.230	0.001
Test5	2.945	3.565	0.094	0.001
Test6	2.980	3.485	0.280	0.001
Test7	2.943	3.687	0.110	0.001
Test8	2.988	3.561	0.690	0.001
Test9	2.979	3.665	0.160	0.001
Test10	2.992	3.506	0.190	0.001
Test11	2.957	2.638	0.001	0.089
Test12	2.987	2.557	0.001	0.092
Test13	2.968	2.731	0.001	1.100
Test14	2.959	2.009	0.001	1.900
Test15	2.989	2.971	0.002	2.900
Test16	2.962	2.769	0.002	5.400
Test17	2.972	2.746	0.003	1.500
Test18	2.955	2.282	0.005	9.900
Test19	2.992	2.224	0.006	1.400

Selection and Validation of Best Hypothesis. The test set consists of 19 molecules, 9 and 10 molecules shows a good selectivity/specificity against Aurora-A and Aurora-B, respectively. The test set was used to validate how well the selected best hypotheses (HypoB1 and HypoA1) can pick the most active inhibitors from least active one as well as to find the selective chemical features which clearly differentiate the Aurora-B inhibitors from Aurora-A. In the test set screening, HypoB1, HypoA1 shows maximum fit values of 3.6 and 2.9, respectively. For the selective and potent inhibitor of Aurora-B and shows the maximum fit values of 2.0 and 2.9 for selective inhibitors of Aurora-A, respectively, indicates that HypoB1 might be best hypothesis to differentiate the Aurora-B from Aurora-A. Comparing the fit values of HypoB1 with the activity values (IC_{50}) of Aurora-B and Aurora-A inhibitors, it clearly represents that HypoB1 establish maximum fit value for a selective Aurora-B inhibitor than Aurora-A inhibitors (Table 5).

HypoB1 was compared with HypoA1 to find the crucial chemical features which can differentiate the Aurora-B

inhibitors form Aurora-A. The remarkable difference is the RA group in HypoB1 hence we propose that this will be important for Aurora-B inhibition. In order to reassert that RA group plays a vital role in the selectivity of Aurora-B inhibitor, we abolished this feature from HypoB1, which represent as HypoB (RA feature in HypoB1 was removed). HypoB was validated by the test set, it shows a similar fit value for Aurora-B and Aurora-A inhibitors which clearly demonstrated that HypoB fails to differentiate Aurora-B inhibitors from Aurora-A. Hence, it was concluded that the RA group could be a key feature to differentiate the Aurora-B from Aurora-A inhibitors. Since HypoB1 shows a good fit value for Aurora-B selective inhibitors than Aurora-A but in the HypoB (absence of RA feature) it shows the fit values equal to that Aurora-A inhibitors. From the above analyses, it was identified that HypoB1 consists all the essential features necessary for compounds to be highly active and selective towards Aurora-B. Hence, the pharmacophore models HypoB1 can be used as a computational tool to design selective Aurora-B inhibitors.

Virtual Screening of Chemical Databases. Another objective of this study is to identify novel scaffold of Aurora-B inhibitors, hence, the best hypothesis, HypoB1, used as 3D query to screen the various chemical databases. Initially HypoB1 screened 20,250 compounds from Maybridge and 16,625 from Chembridge, databases. Following the top 10% from the screened hits were tested for the drug like properties by applying Lipinski's rule of 5 and ADMET properties. According to the rule of five, 1821, and 1662 compounds are selected for further process from Maybridge and Chembridge, respectively. These compounds satisfied the following criteria's such as LogP less than 5, molecular weight less than 500, number of hydrogen bond donors less than 5, number of hydrogen bond acceptors less than 10 and number of rotatable bonds less than 10. The molecular flexibility of molecules, the total number hydrogen bond acceptor and hydrogen bond donors are found to be important predictors for a compound to have a good oral bioavailability. The ADMET properties also calculated using DS, to estimate the values of BBB penetration, solubility, Cytochrome P450 (CYP450), 2D6 inhibition, Hepatotoxicity, Human intestinal adsorption (HIA), Plasma Protein Binding (PPB), and access a broad range of toxicity measure of the ligands. Among all these criteria's we mainly focused on BBB, solubility, and HIA, and the cut off value was 3, 3 and 0, respectively. These are some of the important criteria for a compound to be a good oral bioavailability drug. Based on these criteria's, finally, 182 compounds from Maybridge and 369 from Chembridge databases hits were selected as a drug like compounds. Totally, 664 compounds from two databases were selected for molecular docking study to identify the suitable orientation of hits in the active site of Aurora-B.

Aurora-B 3D Structure Generation Using Homology Modeling Method. Aurora-B plays a critical role in chemogenomic approaches unfortunately the 3D structure of the protein was not crystallized so far, hence using homology

Figure 4. Sequence alignment of template and target sequences using ClustalW.

model 3D structure of Aurora-B was generated. The structure of *Xenopus laevis* Aurora kinase B was selected as suitable template based on Blastp result which shows 77% sequence identity and 6e-130 Evalue. Figure 4 shows the sequence alignment between the template (*Xenopus laevis* Aurora kinase B; PDBID: 2VRX) and the target protein (Homo sapiens Aurora-B) by ClustalW alignment. The final homology model calculation was achieved by Build Homology Models to generate a reliable 3D structure for Human Aurora-B. The full-length Aurora-B has clearly shown the N- and C-terminal domains and the ATP binding cleft was found between these two domains. All β-sheets and α-helices have the similar backbone structure which resembling in *Xenopus laevis* Aurora-B. Aurora-B has the classical bi-lobar protein kinase fold. The N-terminal region is rich in β strands which implicated in nucleotide binding and interacts with kinase regulators. The C-terminal is mainly composed on α helices that act as a docking site for substrates as well as it contain residues that directly play a role in phosphate transfer. The ATP binding pocket was located between the N- and C-terminal regions. Ala173, Glu171, Lys103 and Lys122 and Ala157, Glu155, Glu161 and Lys106 are the critical amino acids in the template protein and Homo sapiens Aurora-B, respectively. Leu122, Glu171 and Asp173 plays a critical role in its function, these are the conserved residues in Aurora-B. The final model was validated using the PROCHECK, to search for deviations from normal protein conformational parameters.

Aurora-B Homology Model Validation. Ramachandran's plot, from PROCHECK, is a protein structure validation program to check the residues-by-residue stereo quality of a protein structure. The phi and psi distributions of the Ramachandran's plot of non-glycine, non-proline residues are shown in Figure 5. Comparing with the template, homology model have a similar Cα conformation, 99.1% of the residues in homology model are found in favored and allowed regions and with a relative low percentage of residues having general torsion angels. A good homology model should show > 90% of the data points in the favorable region supporting that Aurora-B model are sufficiently

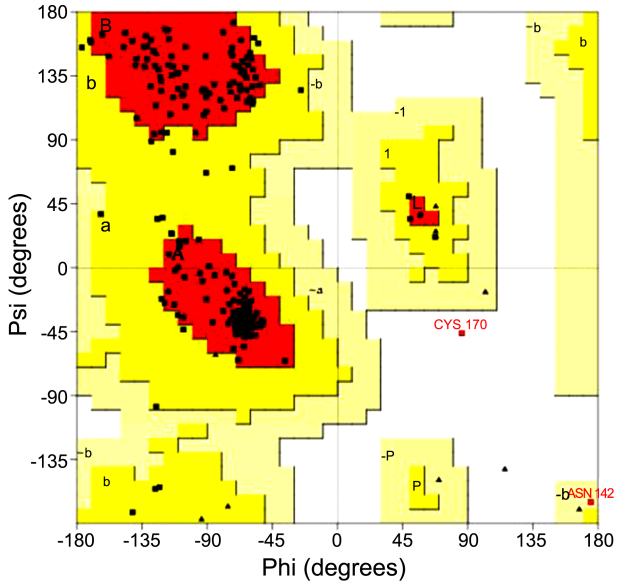

Figure 5. Ramachandran plot's for the homology modeled human Aurora-B.

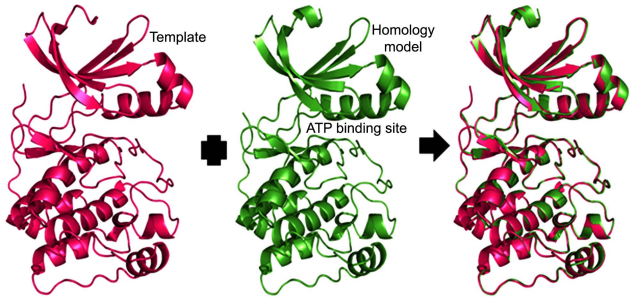

Figure 6. Homology model structure of Aurora-B and comparison with its template structure.

accurate. All bond distances and angles lie within the allowable range about that standard dictionary values which indicated that Aurora-B model is reasonable in geometry and stereochemistry. The root mean square deviation (RMSD) between the template and target structure is 0.073 Å which was shown in Figure 6. The main chain parameters plot for the model showed that the structure compares with well-refined structures at a similar resolution (Fig. 7). The six properties plotted are Ramachandran's plot quality, peptide bond planarity, bad non-bonded interactions, Cá tetrahedral distortion, main chain hydrogen bond energy and the overall G factor which measures the overall normality of the structure. In brief, the geometric quality of the backbone conformation, the residue interaction, the residue contact and the energy profile of the structure are well within the limits established for reliable structures. All the evaluations suggest that a reasonable homology model for Aurora-B has been obtained to allow for examination of protein-substrate interactions.

Molecular Dynamic Simulations. In order to obtain the energetically favorable stable receptor conformation for docking study, after energy minimization, the model was subjected to MD simulation. The RMSD of the protein backbone atoms are plotted as a function of time to check the stability of the system throughout the simulation. During the last 1 ns, the RMSD of each system tends to be converged, indicating the system has been stabilized and well equilibrated. The relative flexibility of the model was characterized by plotting the root mean-square fluctuation (RMSF) relative to the average structure obtained from the MD simulation trajectories. The analyses like RMSD, Potential Energy (PE), and RMSF were carried out to check the stability of the model in explicit condition for 5 ns. Figure 8 shows the overall RMSD analysis of Cá-atoms, which explains the protein structure deviation at atomic level from the initial structure with respect to the function of time. To examine the flexible regions of the model, RMSF plot was generated with respect to their individual residues. The value above 0.4 nm was considered as flexible regions as depicted in Figure 8. The overall analysis of potential energy plot showed a great decline in the energy from the initial energy. A representative structure was obtained from the closest RMSD to the average structure from the last 1 ns MD simulation trajectories was used for further analyses.

Molecular Docking of Aurora-B. Molecular docking was performed using *LigandFit* module to gain insight into the most probable binding conformation of the inhibitors. Molecular docking is a computational technique that samples conformations of small compounds in protein binding sites; scoring functions are used to assess which of these conformations were best complements to the protein binding site. There are two main aspects to assess the quality of docking methods: (i) docking accuracy, which recognizes the true binding mode of the ligands to the target protein and (ii) screening enrichment which measures the relative improvement in the identification of true binding ligands using a docking method versus random screening.

Initially well known 11 specific Aurora-B inhibitors are docked in the active site, to get a clear view about the critical residues present in Aurora-B. The result revealed that Ala157, Glu155, and Lys106 are the critical amino acid plays a major role in Aurora-B hence taking this as criteria to find potent molecules from the virtual screening hits. Totally, 664 hit compounds for all the two databases which all satisfied the drug like properties were docked to investigate their binding mode within active site of Aurora-B. A maximum of 10 poses were saved based on the energy conformation of each molecules. Hydrogen bond analysis was carried out to find how well the molecules stabilized in the active site of Aurora-B. Each poses was checked for possible hydrogen bonds (H-bonds) with critical amino acids present in Aurora-B as well as the occupancy of ligand in the space close to Ala173. Post-docking filter based on H-bond network was constructed to distinguish between active and inactive compounds. Among these compounds only 94 compounds shows the hydrogen bond interactions with Ala157, and either with Glu155 or Lys106. Interestingly, 15 hits (Fig. 9) can form hydrogen bond interactions with three critical residues such as Ala157, Glu155, and Lys106. Two compounds from Maybridge (Compound29545 and

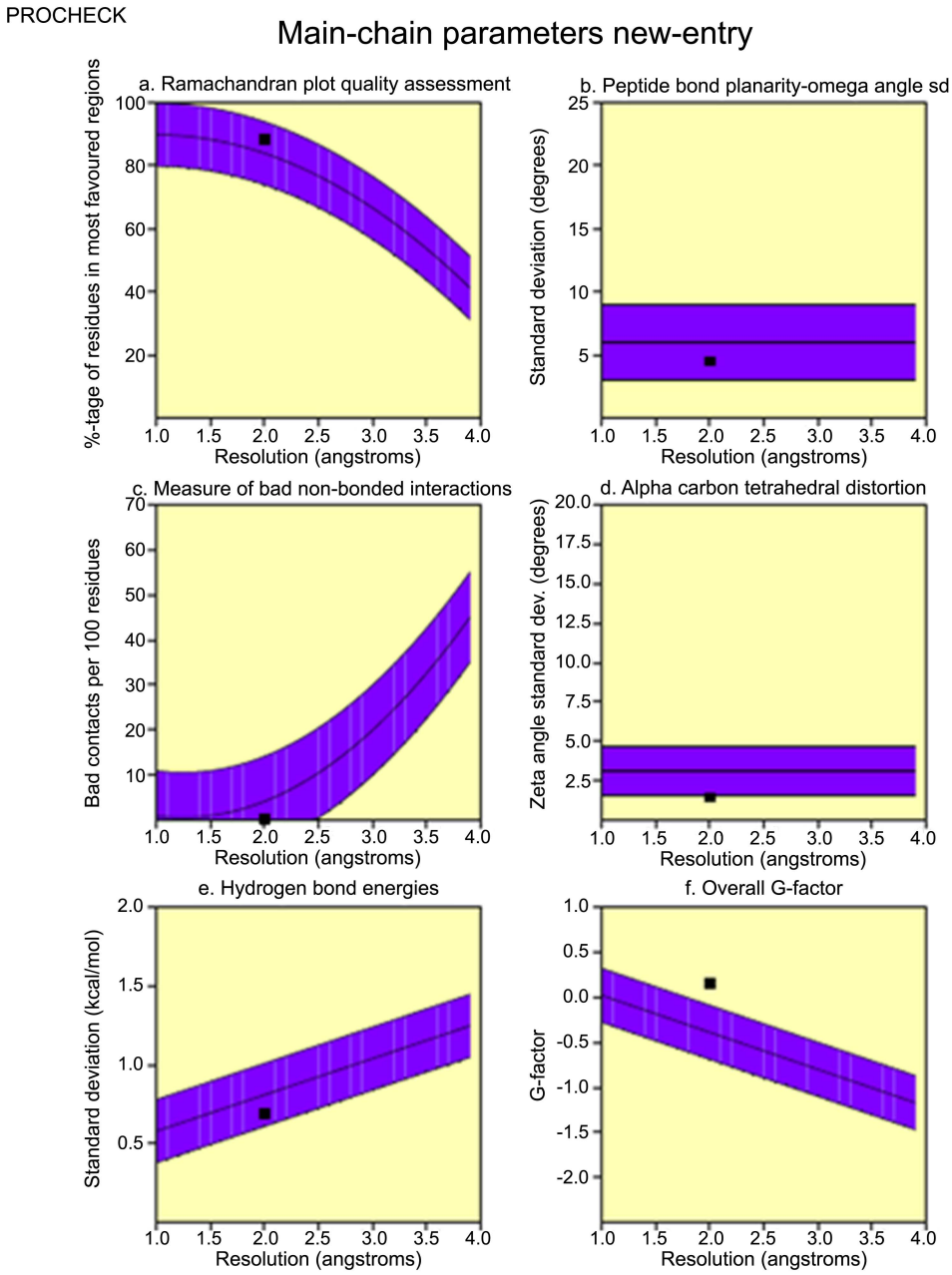

Plot statistics

Stereochemical parameter	No. of data pts	Parameter value	Comparison Values Typical value	Band width	No. of band widths from mean	
a. %-tage residues in A. B. I.	236	88.1	83.8	10.0	0.4	Inside
b. Omega angle st dev	267	4.5	6.0	3.0	-0.5	Inside
c. Bad contacts/100 residues	1	0.4	4.2	10.0	-0.4	Inside
d. Zeta angel st dev	253	1.5	3.1	1.6	-1.0	BETTER
e. H-bond energy st dev	163	0.7	0.8	0.2	-0.6	Inside
f. Overall G-factor	268	0.2	-0.4	0.3	1.8	BETTER

Figure 7. Main chain parameters plot for modeled Aurora-B validated by PROCHECK.

Compound38656) and Chembridge (HTS_09469 and PHG_00530) forms hydrogen bond interactions with Ala157, Glu155, and Lys106 are represented in Fig. 10.

Conclusion

Aurora kinases are one of the emerging drug targets in cancer research field. Qualitative hypotheses were generated for Aurora-A and Aurora-B, to find the selective and critical chemical features which can differentiate the Aurora-B from Aurora-A inhibitors, based on a series of known inhibitors of Aurora-B and Aurora-A. The four and three features hypotheses were selected as a best pharmacophore for Aurora-B (HypoB1) and Aurora-A (HypoA1) based on the

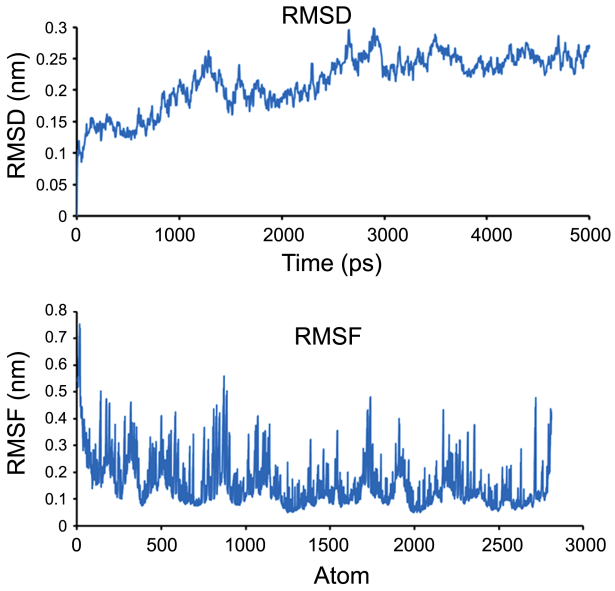

Figure 8. RMSD and RMSF plot of Aurora-B from Molecular Dynamics simulations using GROMACS. Evolution of Cα RMSD from the corresponding initial homology model (b) Root mean square fluctuation (RMSF) of Cα averaged over all subunits from the last 1 ns.

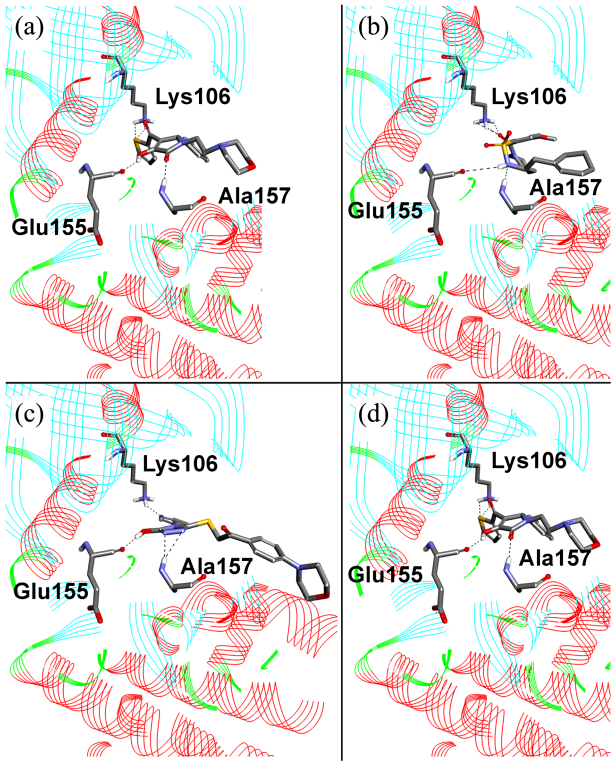

Figure 10. Binding mode of the databases hit molecules in Aurora-B active site (a) Compound29545, (b) Compound38656, (c) HTS_09850 and d) PHG_00530. Hit compounds and the critical residues are shown in stick. Hydrogen bonds are shown in black.

cluster analysis and rank score. These pharmacophore models were validated using the external test set which consist of specific inhibitors of Aurora-B and Aurora-A. The result reveals that HypoB1 and HypoA1 have good capability to separate the Aurora-B from Aurora-A. Compared HypoB1 and HypoA1 to find selective and vital chemical features which can differentiate the selective inhibitors of Aurora-B from Aurora-A. Interestingly, RA group in HypoB1 shows an expected difference when compared with HypoA1. In order to validate the key RA feature, we obliterate this group from HypoB1 hypothesis and validated with the external test sets. But the HypoB (RA group was removed) hypothesis was failed to produced the result as like as HypoB1. Based

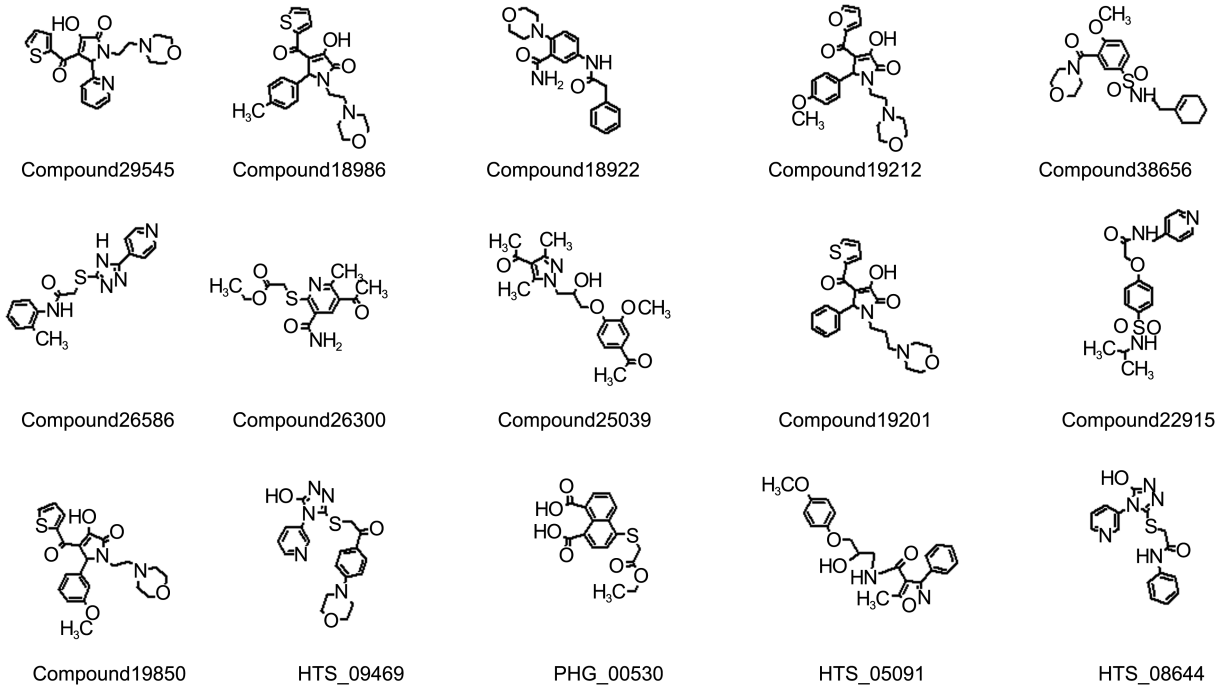

Figure 9. The 2D representation of the 15 hits from Maybridge and Chembridge databases.

on the above results we proposed that the RA group in HypoB1 plays an important role in Aurora-B selectivity. Thus, HypoB1 was used to screen the three different chemical databases such as Maybridge and Chembridge databases. The best hypothesis, HypoB1, screened 20,250, and 16,625 compounds from Maybridge, and Chembridge, respectively. Top 10% from the screened hits were further sorted by applying Lipinski's rule of 5 and ADMET properties. Finally, 664 compounds from two databases were selected for molecular docking study to identify the suitable orientation of hits in the active site of Aurora-B. Homology modeling was executed and the best model was subjected to 5 ns molecular dynamics simulation to analysis the stability of the modeled Aurora kinase-B. The representative structure from the last 1 ns was selected as a receptor for molecular docking studies. Finally, 15 hit compounds for Aurora-B from Maybridge and Chembridge databases shows good hydrogen bond interactions with the critical amino acids such as Ala157, Glu105, and Lys106. Thus, from our results we suggest that HypoB1 will act as a valuable tool for retrieving structurally diverse compounds with desired biological activities and designing novel and selective inhibitors for Aurora kinase B.

Acknowledgments. This research was supported by Basic Science Research Program (2009-0073267), Pioneer Research Center Program (2009-0081539), and Management of Climate change Program (2010-0029084) through the National Research Foundation of Korea (NRF) funded by the Ministry of Education, Science and Technology (MEST) of Republic of Korea. And this work also supported by the Next-Generation BioGreen21 Program (PJ008038) from Rural Development Administration (RDA) of Republic of Korea.

References

1. Girdler, F.; Gascoigne, K. E.; Eyers, P. A.; Hartmuth, S.; Crafter, C.; Foote, K. M.; Keen, N. J.; Taylor, S. S. *Journal of Cell Science* **2006**, *119*, 3664-3675.
2. Mortlock, A. A.; Foote, K. M.; Heron, N. M.; Jung, F. H.; Pasquet, G.; Lohmann, J.-J. M.; Warin, N.; Renaud, F.; De Savi, C.; Roberts, N. J.; Johnson, T.; Dousson, C. B.; Hill, G. B.; Perkins, D.; Hatter, G.; Wilkinson, R. W.; Wedge, S. R.; Heaton, S. P.; Odedra, R.; Keen, N. J.; Crafter, C.; Brown, E.; Thompson, K.; Brightwell, S.; Khatri, L.; Brady, M. C.; Kearney, S.; McKillop, D.; Rhead, S.; Parry, T.; Green, S. *Journal of Medicinal Chemistry* **2007**, *50*, 2213-2224.
3. Qi, M.; Yu, W.; Liu, S.; Jia, H.; Tang, L.; Shen, M.; Yan, X.; Saiyin, H.; Lang, Q.; Wan, B.; Zhao, S.; Yu, L. *Biochemical and Biophysical Research Communications* **2005**, *336*, 994-1000.
4. Carmena, M.; Earnshaw, W. C. *Nature Reviews Molecular Cell Biology* **2003**, *4*, 842-854.
5. Marumoto, T.; Zhang, D.; Saya, H. *Nat. Rev. Cancer* **2005**, *5*, 42-50.
6. Bolanos-Garcia, V. M. *The International Journal of Biochemistry & Cell Biology* **2005**, *37*, 1572-1577.
7. Stephanie, D.; Simon, D.; Claude, P. *Oncogene* **2002**, *21*, 6175-6183.
8. Tsai, M. Y.; Wiese, C.; Cao, K.; Martin, O.; Donovan, P.; Ruderman, J.; Prigent, C.; Zheng, Y. *Nat. Cell Biol.* **2003**, *5*, 242-248.
9. Murata-Hori, M.; Tatsuka, M.; Wang, Y.-L. *Molecular Biology of the Cell* **2002**, *13*, 1099-1108.
10. Kimura, M.; Matsuda, Y.; Yoshioka, T.; Sumi, N.; Okana, Y. *Cytogenet Cell Genet* **1998**, *82*, 147-152.
11. Tang, C.-J. C.; Lin, C. Y.; Tang, T. K. *Developmental Biology* **2006**, *290*, 398-410.
12. Sasai, K.; Katayama, H.; Stenoien, D. L.; Fujii, S.; Honda, R.; Kimura, M.; Okano, Y.; Tatsuka, M.; Suzuki, F.; Nigg, E. A.; Earnshaw, W. C.; Brinkley, W. R.; Sen, S. *Cell Motility and the Cytoskeleton* **2004**, *59*, 249-263.
13. Ikezoe, T. *Cancer Letters* **2008**, *262*, 1-9.
14. Tong, T.; Zhong, Y.; Kong, J.; Dong, L.; Song, Y.; Fu, M.; Liu, Z.; Wang, M.; Guo, L.; Lu, S.; Wu, M.; Zhan, Q. *Clinical Cancer Research* **2004**, *10*, 7304-7310.
15. Katayama, H.; Ota, T.; Jisaki, F.; Ueda, Y.; Tanaka, T.; Odashima, S.; Suzuki, F.; Terada, Y.; Tatsuka, M. *Journal of the National Cancer Institute* **1999**, *91*, 1160-1162.
16. Lee, E. C. Y.; Frolov, A.; Li, R.; Ayala, G.; Greenberg, N. M. *Cancer Research* **2006**, *66*, 4996-5002.
17. Bischoff, J. R.; Anderson, L.; Zhu, Y.; Mossie, K.; Ng, L.; Souza, B.; Schryver, B.; Flanagan, P.; Clairvoyant, F.; Ginther, C.; Chan, C. S. M.; Novotny, M.; Slamon, D. J.; Plowman, G. D. *EMBO J* **1998**, *17*, 3052-3065.
18. Zhou, H.; Kuang, J.; Zhong, L.; Kuo, W. L.; Gray, J. W.; Sahin, A.; Brinkley, B. R.; Sen, S. *Nature Genetics* **1998**, *20*, 189-193.
19. Sen, S.; Zhou, H.; White, R. A. *Oncogene* **1997**, *14*, 2195-2200.
20. Tanaka, T.; Kimura, M.; Matsunaga, K.; Fukada, D.; Mori, H.; Okano, Y. *Cancer Research* **1999**, *59*, 2041-2044.
21. Chieffi, P.; Cozzolino, L.; Kisslinger, A.; Libertini, S.; Staibano, S.; Mansueto, G.; De Rosa, G.; Villacci, A.; Vitale, M.; Linardopoulos, S.; Portella, G.; Tramontano, D. *The Prostate* **2006**, *66*, 326-333.
22. Li, D.; Zhu, J.; Firozi, P. F.; Abbruzzese, J. L.; Evans, D. B.; Cleary, K.; Friess, H.; Sen, S. *Clinical Cancer Research* **2003**, *9*, 991-997.
23. Ke, Y. W.; Dou, Z.; Zhang, J.; Yao, X. B. *Cell Research* **2003**, *13*, 69-81.
24. Marx, J. *Science* **2001**, *292*, 426-429.
25. Carvajal, R. D.; Tse, A.; Schwartz, G. K. *Clinical Cancer Research* **2006**, *12*, 6869-6875.
26. Monaco, L.; Kolthur-Seetharam, U.; Loury, R.; Murcia, J. M.-d.; de Murcia, G.; Sassone-Corsi, P. *Proceedings of the National Academy of Sciences of the United States of America* **2005**, *102*, 14244-14248.
27. Katayama, H.; Sen, S. *Biochimica et Biophysica Acta (BBA) - Gene Regulatory Mechanisms* **1799**, 829-839.
28. Andersen, C. B.; Wan, Y.; Chang, J. W.; Riggs, B.; Lee, C.; Liu, Y.; Sessa, F.; Villa, F.; Kwiatkowski, N.; Suzuki, M.; Nallan, L.; Heald, R.; Musacchio, A.; Gray, N. S. *ACS Chemical Biology* **2008**, *3*, 180-192.
29. Doggrell, S. A. *Expert Opinion on Investigational Drugs* **2004**, *13*, 1199-1201.
30. Fancelli, D.; Moll, J.; Varasi, M.; Bravo, R.; Artico, R.; Berta, D.; Bindi, S.; Cameron, A.; Candiani, I.; Cappella, P.; Carpinelli, P.; Croci, W.; Forte, B.; Giorgini, M. L.; Klapwijk, J.; Marsiglio, A.; Pesenti, E.; Rocchetti, M.; Roletto, F.; Severino, D.; Soncini, C.; Storici, P.; Tonani, R.; Zugnoni, P.; Vianello, P. *Journal of Medicinal Chemistry* **2006**, *49*, 7247-7251.
31. Zhao, B.; Smallwood, A.; Yang, J.; Koretke, K.; Nurse, K.; Calamari, A.; Kirkpatrick, R. B.; Lai, Z. *Protein Science* **2008**, *17*, 1791-1797.
32. Tari, L. W.; Hoffman, I. D.; Bensen, D. C.; Hunter, M. J.; Nix, J.; Nelson, K. J.; McRee, D. E.; Swanson, R. V. *Bioorganic & Medicinal Chemistry Letters* **2007**, *17*, 688-691.
33. Howard, S.; Berdini, V.; Boulstridge, J. A.; Carr, M. G.; Cross, D. M.; Curry, J.; Devine, L. A.; Early, T. R.; Fazal, L.; Gill, A. L.; Heathcote, M.; Maman, S.; Matthews, J. E.; McMenamin, R. L.; Navarro, E. F.; O'Brien, M. A.; O'Reilly, M.; Rees, D. C.; Reule, M.; Tisi, D.; Williams, G.; Vinkovicì, M.; Wyatt, P. G. *Journal of Medicinal Chemistry* **2008**, *52*, 379-388.

34. Rawson, T. E.; Ruth, M.; Blackwood, E.; Burdick, D.; Corson, L.; Dotson, J.; Drummond, J.; Fields, C.; Georges, G. J.; Goller, B.; Halladay, J.; Hunsaker, T.; Kleinheinz, T.; Krell, H.-W.; Li, J.; Liang, J.; Limberg, A.; McNutt, A.; Moffat, J.; Phillips, G.; Ran, Y.; Safina, B.; Ultsch, M.; Walker, L.; Wiesmann, C.; Zhang, B.; Zhou, A.; Zhu, B.-Y.; Ruger, P.; Cochran, A. G. *Journal of Medicinal Chemistry* **2008**, *51*, 4465-4475.
35. Smellie, A.; Teig, S. L.; Towbin, P. *Journal of Computational Chemistry* **1995**, *16*, 171-187.
36. Schormann, N.; Senkovich, O.; Walker, K.; Wright, D. L.; Anderson, A. C.; Rosowsky, A.; Ananthan, S.; Shinkre, B.; Velu, S.; Chattopadhyay, D. *Proteins: Structure, Function, and Bioinformatics* **2008**, *73*, 889-901.
37. Purushottamachar, P.; Khandelwal, A.; Chopra, P.; Maheshwari, N.; Gediya, L. K.; Vasaitis, T. S.; Bruno, R. D.; Clement, O. O.; Njar, V. C. O. *Bioorganic & Medicinal Chemistry* **2007**, *15*, 3413-3421.
38. Doddareddy, M. R.; Jung, H. K.; Lee, J. Y.; Lee, Y. S.; Cho, Y. S.; Koh, H. Y.; Pae, A. N. *Bioorganic & Medicinal Chemistry* **2004**, *12*, 1605-1611.
39. Sakkiah, S.; Thangapandian, S.; John, S.; Lee, K. W. *Journal of Molecular Structure* **2011**, *985*, 14-26.
40. Deng, X.-Q.; Wang, H. Y.; Zhao, Y. L.; Xiang, M. L.; Jiang, P. D.; Cao, Z. X.; Zheng, Y. Z.; Luo, S. D.; Yu, L. T.; Wei, Y. Q.; Yang, S. Y. *Chemical Biology & Drug Design* **2008**, *71*, 533-539.
41. Laskowski, R. A.; MacArthur, M. W.; Moss, D. S.; Thornton, J. M. *Journal of Applied Crystallography* **1993**, *26*, 283-291.
42. Van Der Spoel, D.; Lindahl, E.; Hess, B.; Groenhof, G.; Mark, A. E.; Berendsen, H. J. C. *Journal of Computational Chemistry* **2005**, *26*, 1701-1718.
43. Berendsen, H. J. C.; van der Spoel, D.; van Drunen, R. *Computer Physics Communications* **1995**, *91*, 43-56.
44. Lindahl, E.; Hess, B.; van der Spoel, D. *Journal of Molecular Modeling* **2001**, *7*, 306-317-317.
45. Essmann, U.; Perera, L.; Berkowitz, M. L.; Darden, T.; Lee, H.; Pedersen, L. G. *The Journal of Chemical Physics* **1995**, *103*, 8577-8593.
46. Hess, B.; Bekker, H.; Berendsen, H. J. C.; Fraaije, J. G. E. M. *Journal of Computational Chemistry* **1997**, *18*, 1463-1472.
47. Berendsen, H. J. C.; Postma, J. P. M.; van Gunsteren, W. F.; DiNola, A.; Haak, J. R. *J. Chem. Phys.* **1984**, *81*, 3684-3690.